Synchronized closed path following for a differential drive and manipulator robot

Yuqian Li and Christopher Nielsen *Member, IEEE*

Li, Y., & Nielsen, C. (2017). Synchronized Closed Path Following for a Differential Drive and Manipulator Robot. IEEE Transactions on Control Systems Technology, 25(2), 704–711. https://doi.org/10.1109/TCST.2016.2562578

***Abstract*—We locally solve a synchronized path following problem for a heterogenous multi-agent system consisting of a differential drive robot and a serial manipulator. Each is assigned a simple, regular, closed curve in its output space. The outputs of the systems must approach and traverse their assigned curves while synchronizing their motions along the paths. We use the notion of path following outputs to facilitate a solution and present a novel synchronization controller and a novel singularity avoidance controller. The controllers are all given in closed-form making their implementation straightforward. A numerical simulation is presented which includes modelling uncertainty to demonstrate the utility of this approach.**

I. Introduction

Flexible manufacturing systems have the ability to quickly change their workflow over time. For example, Amazon.com Inc. has successfully used teams of mobile robots and robotic manipulators to automate its warehouse operations. Consider a scenario where (i) a robotic manipulator picks up a part and (ii) places it on a mobile robot which (iii) delivers the part to a station to be processed and (iv) the scenario repeats indefinitely. In this scenario, the manipulator's end effector and the mobile robot should each traverse an appropriately planned closed curve in order to repeatedly pick up and deliver parts. The traversal of the curves should be very accurate to avoid collisions with other stations. Finally, the machines should be synchronized so that neither of the robots are waiting.

Partially motivated by the scenarios like the one above, this paper focuses on a synchronized path following problem for closed paths and a heterogenous multi-agent system consisting of a differential drive robot and a serial manipulator. Path following refers to the problem of driving the output of a system to a pre-assigned path with no *a priori* time parameterization of the motion along the path. This distinguishes path following from trajectory tracking and allows path following controllers to remove performance limitations for non-minimum phase systems [1] and to enforce path invariance [2]. Path invariance means that path following controllers are able to stabilize *all* the motions of a system whose associated output trajectory lies on the assigned path.

For a multi-robot system, coordinated path following entails making each robot approach a pre-assigned path, again, with no *a priori* time parameterization. Once on the paths, the robots should coordinate. This could mean various things depending on the application. The robots may be required to: keep a desired inter-vehicle formation pattern in time [3], [4], [5]; get into formation and then move along straight lines [6]; or to get their path variables, the variable that describes where a robot is on its path, to converge to a common value [7]. These papers all share the property that synchronization is enforced through a clever re-parameterization of the assigned paths. Once the re-parameterization is obtained, the synchronization problem reduces to a consensus problem [8].

We take an invariant sets approach to the coordinated path following problem [9] and view the problem as an instance of hierarchical control [10]. This means that our controllers first stabilize all the motions of the robots whose associated output signals belong to the assigned path. Synchronization is modeled by a function whose zero level set constrains the allowable motions along the paths. Synchronization is achieved by stabilizing the zero level set of this function. By using a constraint function, we achieve at least three things that make this approach unique. First, we do not need to cleverly re-parameterize the paths to frame the synchronization problem as a consensus problem. Second, we achieve synchronization invariance. This is accomplished by stabilizing *all* the trajectories of the team for which the synchronization constraint is satisfied. In other words, if the robots are traversing their paths in a synchronized manner and we decide to change, say, the velocity of the synchronized team, they will converge to the new velocity profile without falling out of synchronization nor leaving their paths. Thirdly, using this constraint function allows us to achieve more general forms of synchronization than just maintaining a formation. These features are unique to path following as opposed to synchronization using a tracking approach [11], [12].

While our approach is based on [9], this paper has several key differences[1]. We consider a heterogenous team of robots that do not have identical dynamics. We introduce a novel singularity avoidance controller for differential drive robots that extends the applicability of the results in [9]. An explicit characterization of synchronization functions is provided. Furthermore, by focusing on the special case of two robots and closed-paths, we are able to obtain a closed-form expression for our synchronization controller that is applicable to relative degree two systems. We also present a closed-form expression for a controller that allows the positionally synchronized system to track a velocity profile.

Partially supported by the Natural Sciences and Engineering Research Council of Canada (NSERC).

The authors are with the Department of Electrical and Computer Engineering, University of Waterloo, 200 University Avenue West, Waterloo, Ontario, Canada, N2L 3G1. {y433li;cnielsen}@uwaterloo.ca

[1]A preliminary version of this paper appeared in [13]. The paper has a completely different singularity avoidance controller (Section IV), we present an improved synchronization controller that does not require a leader (Section VI) and more robust simulations with model uncertainty are provided.

A. Notation

Given vectors $x, y \in \mathbb{R}^n$, $\langle x,\ y\rangle$ denotes the Euclidean inner product and $\|x\|$ the associated Euclidean norm. For a set $A \subset \mathbb{R}^n$, the point-to-set distance is written $\|\cdot\|_A$. Given $n \in \mathbb{N}$, $\mathbf{n} := \{1, \ldots, n\}$. If $L > 0$ and real, then the notation $\mathbb{R} \bmod L$ represents the real numbers modulo L and $[\cdot]_L : \mathbb{R} \to \mathbb{R} \bmod L$. Let $\arg : \mathbb{C} \to (-\pi, \pi]$ map a complex number to its principal argument. The symbol $\otimes$ denotes the Kronecker product while $:=$ means equal by definition.

For a function $\sigma : A \to B$, $\mathrm{Im}(\sigma)$ denotes its image. The function σ is proper if the pre-image of every compact set in B is compact in A where A and B are topological spaces. If $\phi : \mathbb{R}^n \to \mathbb{R}^m$ is a smooth map, $\mathrm{d}\phi_x$ denotes its Jacobian evaluated at x and $\mathrm{Hess}\,(\phi)$ is its Hessian matrix. If $f,\ g : \mathbb{R}^n \to \mathbb{R}^n$ are smooth vector fields, we use the following standard notation for iterated Lie derivatives $L_f^0\phi(x) := \phi(x)$, $L_f^k\phi(x) := L_f(L_f^{k-1}\phi)(x) = \langle \mathrm{d}L_f^{k-1}\phi_x, f(x)\rangle$, $L_gL_f\phi(x) := L_g(L_f\phi)(x) = \langle \mathrm{d}L_f\phi_x, g(x)\rangle$.

II. Problem formulation

We consider a synchronized path following problem for two different nonlinear, control-affine, deterministic control systems. System Σ_a is taken to be a differential drive robot. Differential drive, i.e., type $(2,0)$ mobile robots [14], are commonly called unicycle robots. Its state vector is $x_a := (x_1, x_2, x_3, x_4)$ (see Figure 1). Translational and rotational accelerations are the control inputs. The resulting model has the form $\dot{x}_a = f(x_a) + g_1(x_a)u_{1,a} + g_2(x_1)u_{2,a}$;

$$\dot{x}_a = \begin{bmatrix} x_4\cos x_3 \\ x_4 \sin x_3 \\ 0 \\ 0 \end{bmatrix} + \begin{bmatrix} 0 \\ 0 \\ 0 \\ 1 \end{bmatrix} u_{1,a} + \begin{bmatrix} 0 \\ 0 \\ 1 \\ 0 \end{bmatrix} u_{2,a}. \tag{1}$$

The robot's position in the plane is taken as its output $y_a = h_a(x_a) = (x_1, x_2)$. Let $p_a := 2$ denote the dimension of y_a and let $\tau(x_3) := (\cos(x_3), \sin(x_3))$ denote the unicycle's heading direction.

System Σ_b is taken to be a fully actuated serial manipulator with a 4-dimensional configuration space $\mathbb{R}^4$ and 4 control inputs $\tau \in \mathbb{R}^4$. The dynamic model is given in standard vector form as

$$M(q)\ddot{q} + C(q,\dot{q})\dot{q} + G(q) = B(q)\tau \tag{2}$$

where the symmetric inertia matrix $M(q)$ is positive definite for all q and $B : \mathbb{R}^4 \to \mathbb{R}^{4\times 4}$ is smooth, non-singular for all q. We take the position of the robot's wrist in the task space as the output

$$y_b = h_b(q), \qquad h_b : \mathbb{R}^4 \to \mathbb{R}^3. \tag{3}$$

Let $p_b := 3$ denote the dimension of y_b. The closed-form expression of (3) is omitted but can be computed using standard methods for forward kinematics.

We now describe the class of paths considered. Let $i \in \{a, b\}$ and let $\mathcal{C}_i$ be a simple, regular, closed curve of length $L_i > 0$ in the output space of system Σ_i with smooth unit speed parameterization $\sigma_i : \mathbb{R} \to \mathbb{R}^{p_i}$, $\mathrm{Im}\,(\sigma_i) = \mathcal{C}_i$, $\|\sigma_i'(\cdot)\| \equiv 1$.

Assumption 1 (implicit representation)**.** *The regular closed curves $\mathcal{C}_i \subset \mathbb{R}^{p_i}$, $i \in \{a, b\}$, have implicit representations*

$$\mathcal{C}_i = \{y_i \in W_i \subseteq \mathbb{R}^{p_i} : s_i(y_i) = 0\}$$

where $s_i : W_i \subseteq \mathbb{R}^{p_i} \to \mathbb{R}^{p_i - 1}$ are smooth functions such that $\mathrm{rank}\,(\mathrm{d}s_i) = p_i - 1$ on $\mathcal{C}_r$ and W_i are open sets containing $\mathcal{C}_i$.

Assumption 1 automatically holds if $p_i \in \{2, 3\}$, as in our case, or if the parameterizations are regular of order p_i. Our control objective is to design feedback control laws that make the closed-loop output of Σ_i approach the curve $\mathcal{C}_i$ and synchronize their motion. To make our notion of synchronization precise, we introduce a synchronization constraint.

Definition II.1. *A **path following synchronization constraint** for two systems Σ_i and curves $\mathcal{C}_i \subset \mathbb{R}^{p_i}$, $i \in \{a, b\}$ is a relation $F(y_a, \dot{y}_a, y_b, \dot{y}_b) = 0$ where $F : \mathcal{C}_a \times \mathbb{R}^{p_a} \times \mathcal{C}_b \times \mathbb{R}^{p_b} \to \mathbb{R}^k$ is smooth, $k \in \mathbf{4}$, and $\mathrm{rank}\,(\mathrm{d}F) = k$ on $F^{-1}(0)$.*

Synchronized path following problem (SPFP) : Given two regular closed curves $\mathcal{C}_a$ and $\mathcal{C}_b$ satisfying Assumption 1, and a path following synchronization constraint $F : \mathcal{C}_a \times \mathbb{R}^{p_a} \times \mathcal{C}_b \times \mathbb{R}^{p_b} \to \mathbb{R}^k$, find control laws $u_a : \mathbb{R}^{n_a} \times \mathbb{R}^{n_b} \to \mathbb{R}^{m_a}$, $u_b : \mathbb{R}^{n_a} \times \mathbb{R}^{n_b} \to \mathbb{R}^{m_b}$ such that, for an open set of initial conditions $\mathcal{X}_a \subseteq \mathbb{R}^{n_a}$, $\mathcal{X}_b \subseteq \mathbb{R}^{n_b}$ with $\mathcal{C}_a \subset h_a(\mathcal{X}_a)$, $\mathcal{C}_b \subset h_b(\mathcal{X}_b)$, the closed-loop systems satisfy

- **A** (Attractivity) The solutions $x_a(t)$, $x_b(t)$ satisfy $\|h_a(x_a(t))\|_{\mathcal{C}_a} \to 0$ and $\|h_b(x_b(t))\|_{\mathcal{C}_b} \to 0$ as $t \to \infty$.
- **I** (Invariance) The curves $\mathcal{C}_a$ and $\mathcal{C}_b$ are output invariant for the respective closed-loop systems.
- **S** (Synchronization) If, for all $t \geq 0$, $h_a(x_a(t)) \in \mathcal{C}_a$, $h_b(x_b(t)) \in \mathcal{C}_b$, then $F(y_a(t), \dot{y}_a(t), y_b(t), \dot{y}_b(t)) \to 0$ as $t \to \infty$.

$\Diamond$

Objective **A** in SPFP asks that the assigned paths be attractive for the closed-loop systems. Objective **I** asks that the assigned paths be invariant in the sense that, if the closed-loop systems are properly initialized, the corresponding solutions evolve on their assigned paths irrespective of the synchronization specification. Finally, objective **S** asks that the systems synchronize their motion along the path.

Remark II.2. *We have expressed **S** as a constraint on the allowable motions on the curve in accordance with Definition II.1. In practice, condition **S** must also hold for solutions that asymptotically approach the curves. The more practical scenario is studied using an appropriately defined projection onto the curves (see (4) and Section VI).*

III. Path following outputs

Let Σ be a control affine system assigned a simple closed curve in the class described in Section II. Let $\alpha : U \subseteq \mathbb{R}^n \to \mathbb{R}^{p-1}$ $x \mapsto s \circ h(x)$ where $U := s^{-1}(W)$ and $s(\cdot)$, $W \subseteq \mathbb{R}^p$ are defined in Assumption 1. The function $\alpha(\cdot)$ has the property that if $h(x) \in \mathcal{C}$ then $\alpha(x) = 0$. This property allows one to treat the problem of driving the output of Σ towards $\mathcal{C}$ as an output stabilization problem. Intuitively, one can view $s(\cdot)$ as

a signed distance function from the system output to the path and the problem of getting on the path as being the problem of driving this distance to zero.

Additionally, let $\pi : U \subseteq \mathbb{R}^n \to \mathbb{R}$ be defined as $x \mapsto \varpi \circ h(x)$ where

$$\begin{aligned} \varpi : \mathcal{N}(\mathcal{C}) \subset \mathbb{R}^p &\to \mathbb{R} \bmod L \\ y &\mapsto \underset{\lambda \in [0,L)}{\arg\min} \|y - \sigma(\lambda)\|. \end{aligned} \tag{4}$$

The function (4) returns the parameter $\lambda \in [0, L)$ that minimizes the distance from the output to the path. It is well-defined in a neighbourhood $\mathcal{N}(\mathcal{C})$ of the curve $\mathcal{C}$. The function π has the property that, for all $x_1, x_2 \in \mathbb{R}^n$ such that $h(x_1), h(x_2) \in \mathcal{C}$ and $\pi(x_1) \neq \pi(x_2)$ then $h(x_1) \neq h(x_2)$. This makes it a useful function for controlling the motion of the system on the curve. The following definition summarizes this discussion.

Definition III.1. *The **path following output** of a control system Σ with respect to a closed curve $\mathcal{C}$ satisfying Assumption 1 is*

$$y_{\text{PF}} \coloneqq \begin{bmatrix} \alpha(x) \\ \pi(x) \end{bmatrix}. \tag{5}$$

*The **path following manifold** [2], denoted $\Gamma^\star$, with respect to $\mathcal{C}$ is the largest controlled invariant subset of $\alpha^{-1}(0)$.*

Lemma III.2. *The dynamic unicycle (1) with path following output (5) yields a well-defined vector relative degree of $\{r_1, r_2\} = \{2, 2\}$ at each point on $h_a^{-1}(\mathcal{C}_a)$ at which $x_4 \neq 0$.*

The proof of Lemma III.2 is omitted. By Lemma III.2, in a neighbourhood of every point in the open set $\{x \in \mathbb{R}^4 : \alpha_a(x) = 0\} \setminus \{x_a : x_4 = 0\}$ the unicycle system is feedback equivalent to

$$\begin{aligned} \dot\eta_1^a &= \eta_2^a \quad \dot\xi_1^a = \xi_2^a \\ \dot\eta_2^a &= v_a^{\shortparallel} \quad \dot\xi_2^a = v_a^{\pitchfork}. \end{aligned} \tag{6}$$

The path following manifold of the unicycle (1) with respect to the curve $\mathcal{C}_a$ is $\Gamma_a^\star = \{x_a \in \mathbb{R}^4 : \alpha_a(x) = L_f\alpha_a(x) = 0\} = \{x_a \in \mathbb{R}^4 : \xi_1^a = \xi_2^a = 0\}$ and has dimension two.

In the case of the manipulator (2), (3), if we augment the path following output with a fourth artificial output $\phi(q) \coloneqq q_2 + q_3 + q_4$, then the output (y_{PF}, ϕ) yields a relative degree of $\{2, 2, 2, 2\}$ away from kinematic singularities. Hence the 4-DOF manipulator is feedback equivalent, in a neighbourhood of every point on the path $\mathcal{C}_b$, to

$$\begin{aligned} \dot\zeta_1^b &= \zeta_2^b \quad \dot\eta_1^b = \eta_2^b \quad \dot\xi_1^1 = \xi_2^1 \quad \dot\xi_1^2 = \xi_2^2 \\ \dot\zeta_2^b &= v^\zeta \quad \dot\eta_2^b = v_b^{\shortparallel} \quad \dot\xi_2^1 = v_{b,1}^{\pitchfork} \quad \dot\xi_2^2 = v_{b,2}^{\pitchfork}. \end{aligned} \tag{7}$$

The path following manifold of the manipulator (1) with respect to the curve $\mathcal{C}_b$ is $\Gamma_b^\star = \{x_b \in \mathbb{R}^8 : \xi_j^i = 0, i, j \in \mathbf{2}\} = \{x_b \in \mathbb{R}^8 : \alpha_b(x) = L_f\alpha_b(x) = 0\}$ and has dimension 4. The ζ^b states, which model redundant dynamics, play no role in the SPFP. We hereafter set $v^\zeta = K_\zeta \zeta$ to exponentially stabilize $(\zeta_1^b, \zeta_2^b) = (0, 0)$.

IV. Switching through singularities

Lemma III.2 shows that the path following output does not yield a well-defined vector relative degree for (1) when $x_4 = 0$. In order for the unicycle to synchronize with (2), it may have to stop or turn around on its path which can result in zero translational velocity. In this section we propose a scheme that avoids this singularity. We partition the state space of the unicycle into two regions. Let $\delta > 0$ be a fixed constant and define $M_\delta \coloneqq \{x_a : \|(x_4, \xi^a)\| < \delta\}$ and $M \coloneqq \{x_a : \|(x_4, \xi^a)\| \geq \delta\}$. The set M_δ corresponds to the unicycle's translational velocity being small (small x_4), it's position close to $\mathcal{C}_a$ (small ξ_1^a) and its heading almost tangent to $\mathcal{C}_a$ (small ξ_2^a). When $x_a \in M$, we apply the feedback transformation that yields (6). When $x_a \in M_\delta$, we instead apply [14] the coordinate transformation $\Psi : \mathbb{R}^4 \to \mathbb{R}^4$

$$\begin{bmatrix} \eta_1^a \\ \eta_2^a \\ \ell \\ \theta \end{bmatrix} = \begin{bmatrix} \pi_a(x_a) \\ L_f\pi_a(x_a) \\ \left\langle R_{\frac{\pi}{2}}\sigma_a'(\lambda^\star),\ h_a(x_a) - \sigma_a(\lambda^\star) \right\rangle \\ \arg\left(\mathrm{e}^{j(x_3 - \varphi(\lambda^\star))}\right) \end{bmatrix} \tag{8}$$

where $\lambda^\star = \pi_a(x_a)$ is the value returned by (4) and $\varphi : \mathbb{R} \bmod L_a \to \mathbb{R} \bmod 2\pi$ is the map associating to each $\lambda \in [0, L_a)$ the angle of the tangent vector $\sigma_a'(\lambda)$ to $\mathcal{C}_a$ at $\sigma(\lambda)$. The states (ℓ, θ) represent the signed distance from the unicycle to its path and its orientation error, see Figure 1.

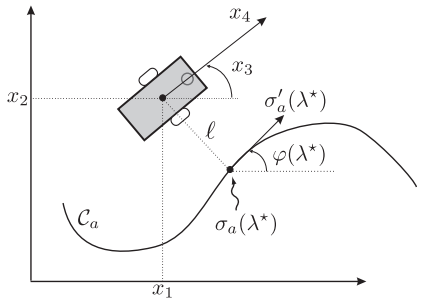

Fig. 1: Physical meaning of the states ℓ and θ.

Proposition IV.1. *For every $\overline{x}_a \in \Gamma_a^\star$, there exists an open set $U \subset \mathbb{R}^4$ containing $\overline{x}_a$ such that (8) is a local diffeomorphism.*

Proof. The Jacobian of Ψ evaluated at $\overline{x}_a \in \Gamma_a^\star$ has the form

$$\mathrm{d}\Psi(\overline{x}_a) = \begin{bmatrix} \frac{\partial \pi_a}{\partial x_1} & \frac{\partial \pi_a}{\partial x_2} & 0 & 0 \\ \frac{\partial L_f\pi_a}{\partial x_1} & \frac{\partial L_f\pi_a}{\partial x_2} & \frac{\partial L_f\pi_a}{\partial x_3} & \frac{\partial L_f\pi_a}{\partial x_4} \\ \frac{\partial \ell}{\partial x_1} & \frac{\partial \ell}{\partial x_2} & 0 & 0 \\ \frac{\partial \theta}{\partial x_1} & \frac{\partial \theta}{\partial x_2} & 1 & 0 \end{bmatrix}.$$

To show that $\mathrm{d}\Psi$ is non-singular, we argue that (i) the (2, 4)-entry is non-zero and (ii) rows one and three are linearly independent. Simple calculations yield

$$\frac{\partial L_f\pi_a}{\partial x_4} = L_{g_1}L_f\pi_a = \frac{\langle \sigma_a'(\lambda^\star),\ \tau(x_3)\rangle}{\|\sigma_a'(\lambda^\star)\|} = \langle \sigma_a'(\lambda^\star),\ \tau(x_3)\rangle.$$

On $\Gamma_a^\star$, the unicycle is on the path and its heading is tangent to the path and therefore $\langle \sigma_a'(\lambda^\star),\ \tau(x_3)\rangle = \pm 1$.

Next, we show that rows one and three are linearly independent. To begin with, write the first and third components

of Ψ as compositions $\psi_1(x_a) = \varpi_a \circ h_a(x_a)$, $\psi_3(x_a) = \gamma \circ h_a(x_a)$. Applying the chain rule $\mathrm{d}\psi_1 = \mathrm{d}(\varpi_a)_{h_a(x_a)}\mathrm{d}h_a(x_a)$, $\mathrm{d}\psi_3 = \mathrm{d}\gamma_{h_a(x_a)}\mathrm{d}h_a(x_a)$ and so it is sufficient to show that $\mathrm{d}(\varpi_a)_{y_a}$ and $\mathrm{d}\gamma_{y_a}$ are linearly independent. This fact follows from [15, Lemma 3.2] which shows that $\nabla\varpi_a = \mathrm{d}(\varpi_a)_{y_a}^\top$ and $\nabla\gamma = \mathrm{d}\gamma_{y_a}^\top$ are orthogonal. □

The unicycle (1) under the coordinate transformation (8) is given by [14]

$$\begin{aligned}\dot\eta_1^a &= \eta_2^a\\ \dot\eta_2^a &= L_f^2\pi_a + L_{g_1}L_f\pi_a u_{1,a} + L_{g_2}L_f\pi_a u_{2,a}\\ \dot\ell &= x_4\sin(\theta)\\ \dot\theta &= u_{2,a} - x_4\cos(\theta)\tfrac{\kappa(\eta_1^a)}{1-\kappa(\eta_1^a)\ell}\end{aligned}$$

where $x_a = \Psi^{-1}(\eta^a, \ell, \theta)$ and $\kappa : \mathbb{R} \bmod L_a \to \mathbb{R}$ is the signed curvature function of $\mathcal{C}_a$. Consider the feedback transformation

$$\begin{bmatrix} u_{1,a}\\ u_{2,a}\end{bmatrix} = \tilde\beta(x_a)^{-1}\left(\begin{bmatrix} -L_f^2\pi_a\\ x_4\cos(\theta)\frac{\kappa(\eta_1^a)}{1-\kappa(\eta_1^a)\ell}\end{bmatrix} + \begin{bmatrix} v_a^{\parallel}\\ v_\delta^{\pitchfork}\end{bmatrix}\right) \tag{9}$$

with

$$\tilde\beta(x_a) := \begin{bmatrix} L_{g_1}L_f\pi_a & L_{g_2}L_f\pi_a\\ 0 & 1\end{bmatrix}.$$

Corollary IV.2. *The feedback transformation (9) is well defined at every $\overline{x}_a \in \Gamma_a^\star$.*

Proof. The determinant of $\tilde\beta(x_a)$ is $L_{g_1}L_f\pi_a(x_a)$ which, as shown in the proof of Proposition IV.1, equals $\langle\sigma_a'(\lambda^\star),\ \tau(x_3)\rangle = \pm 1$ at $\overline{x}_a \in \Gamma_u^\star$. □

The proof of Corollary IV.2 illustrates that, when the heading vector $\tau(x_3)$ is orthogonal to the path, feedback (9) is not well-defined. This observation helps motivate the definition of M_δ since we only switch to (9) when the unicycle is almost tangent to the path. After applying (9), the unicycle model is

$$\begin{aligned}\dot\eta_1^a &= \eta_2^a \quad \dot\ell = x_4\sin(\theta)\\ \dot\eta_2^a &= v_a^{\parallel} \quad \dot\theta = v_\delta^{\pitchfork}.\end{aligned} \tag{10}$$

V. Attractivity and Invariance of the Paths

The unicycle's normal form (6) and the manipulator's normal form (7) are useful for solving SPFP. When the ξ^i, $i \in \{a, b\}$, states are zero the systems evolve on their respective path following manifolds. As such the ξ^i-dynamics govern that portion Σ_i's dynamics that move it towards or away from the assigned curve; we call them transversal dynamics. Since these dynamics are linear and controllable, objectives **A** and **I** of SPFP can be solved using linear feedback. The simplest choice of transversal controllers are

$$v_a^{\pitchfork} = K_a\xi^a, \qquad v_b^{\pitchfork} = K_b\xi^b \tag{11}$$

where the real gains K_a, K_b are selected so that the closed-loop matrices are Hurwitz. The LTI controllers (11) make the equilibrium points $\xi^i = 0$ of the closed-loop transversal subsystems exponentially stable. Physically this implies that if the systems are initialized on their paths with a velocity tangent to the path, then they remain on the path for all future time. Therefore, path invariance **I** is achieved. Furthermore, if the closed-loop trajectories are bounded, then $\xi^a, \xi^b \to 0$ implies that $x_a \to \Gamma_a^\star$, $x_b \to \Gamma_b^\star$ which means that the paths are attractive (objective **A**).

There is an additional complication for the unicycle because it is not feedback equivalent to (6) when $x_4 = 0$. To overcome this problem we employ the results of Section IV. When $x_b \in M_\delta$, the unicycle is feedback equivalent to (10). By the physical meaning of (ℓ, θ) (see Figure 1) we conclude that $\xi_1^a = \xi_2^a = 0$ if, and only if, $\ell = 0$ and $\theta \in \{0, \pi\}$.

We now design the input $v_\delta^{\pitchfork}$ such that if a singularity is encountered near the path following manifold the unicycle does not leave its path. Our controller uses the smooth bump function $\mathbb{R} \to \mathbb{R}$

$$\mathrm{bump}_{(K,A,c)}(\theta) = K\left(\frac{1}{h(A)^2}h(\theta + A)\,h(A - \theta) + c\right) \tag{12}$$

with

$$h(\theta) = \int_{-\infty}^{\theta} f(\tau+1)f(1-\tau)\mathrm{d}\tau, \quad f(\tau) = \begin{cases}\mathrm{e}^{-\frac{1}{\tau}} & \tau > 0\\ 0 & \tau \le 0.\end{cases}$$

The constant $A > 0$ determines the width of the bump; $c \in \mathbb{R}$ determines the offset; $K \in \mathbb{R}$ is a scaling factor.

Proposition V.1. *System (10) with*

$$\begin{aligned}v_\delta^{\pitchfork} = &-b_1^0(\theta)x_4\ell\,\mathrm{sinc}(\theta) - b_1^\pi(\theta)x_4\ell\,\mathrm{sinc}([\theta]_{2\pi} - \pi)\\ &- b_2(\theta)|x_4|\sin(\theta)\end{aligned} \tag{13}$$

where

$$\begin{aligned}b_1^0(\theta) &= \mathrm{bump}_{(K_1,\pi/2,0)}(\theta), \quad b_1^\pi(\theta) = \mathrm{bump}_{(K_1,\pi/2,-1)}(\theta)\\ b_2(\theta) &= \mathrm{bump}_{(2K_2,\pi/2,-0.5)}(\theta), \quad K_1, K_2 > 0\end{aligned} \tag{14}$$

enjoys the following properties.

(i) *The set $\Gamma_a^\star$ is controlled invariant.*
(ii) *The equilibria $(\ell, \theta) = (0, 0)$, $(\ell, \theta) = (0, \pi)$ of the (ℓ, θ)-subsystem are stable.*
(iii) *If $\liminf_{t\to\infty}|x_4| \neq 0$ then $(\ell, \theta) = (0, 0)$ and $(\ell, \theta) = (0, \pi)$ are locally asymptotically stable.*

Proof. To prove (i) let $x_a \in \Gamma_a^\star = \{x_a : \xi^a = 0\}$. By the definitions of (ℓ, θ) and $\Gamma_a^\star$, $\xi^a = 0$ if and only if $\ell = 0$ and $\theta \in \{0, \pi\}$. Both $(\ell, \theta) = (0, 0)$ and $(\ell, \theta) = (0, \pi)$ are equilibria of the (ℓ, θ)-subsystem of (10) under the feedback (13) which shows that (i) holds.

To prove (ii) let[2] $U_0 := \{(\ell, \theta) : |\theta| < 0.5\}$. On this set $b_1^0(\theta) = K_1$, $b_1^\pi(\theta) = 0$ and $b_2(\theta) = K_2$ so that (13) reduces to

$$v_\delta^{\pitchfork} = -K_1x_4\ell\,\mathrm{sinc}(\theta) - K_2|x_4|\sin(\theta).$$

Next consider the candidate Lyapunov-like function $V : \mathbb{R} \times U_0 \to \mathbb{R}$, $V(\ell, \theta) = K_1\frac{\ell^2}{2} + \frac{\theta^2}{2}$. The time derivative of V along the (l, θ)-subsystem gives

$$\begin{aligned}\dot V &= K_1\ell x_4\sin(\theta) - K_1\theta x_4\ell\,\mathrm{sinc}(\theta) - K_2\theta|x_4|\sin(\theta)\\ &= -K_2\theta|x_4|\sin(\theta) \le 0.\end{aligned}$$

[2]The set U_0 depends on the choice of the parameter A in (12) but the stated value is valid for the choices made in (14).

which shows that $(\ell,\theta) = (0,0)$ is stable and $\Omega_0 := \sup_{c\geq 0} V^{-1}(c)$ such that $\Omega_0 \subset \mathbb{R}\times U_0$ is a compact positively invariant set. To show that $(\ell,\theta) = (0,\pi)$ is also stable let $U_\pi := \{(\ell,\theta) : |\theta| > \pi - 0.5\}$ and consider the smooth function $V : \mathbb{R}\times U_\pi \to \mathbb{R}$, $V(\ell,\theta) = K_1\frac{\ell^2}{2} + ([\theta]_{2\pi} - \pi)^2/2$. On U_π, $b_1^0(\theta) = 0$, $b_1^\pi(\theta) = K_1$ and $b_2(\theta) = -K_2$ so that (13) reduces to

$$v_\delta^{\pitchfork} = K_1 x_4 \ell\, \mathrm{sinc}\left([\theta]_{2\pi} - \pi\right) + K_2|x_4|\sin(\theta).$$

The derivative of V, for $(\ell,\theta)\in\mathbb{R}\times U_\pi$, satisfies

$$\begin{aligned}\dot V &= K_1\ell x_4 \sin(\theta) + K_1\left([\theta]_{2\pi} - \pi\right) x_4 \ell\, \mathrm{sinc}\left([\theta]_{2\pi} - \pi\right)\\ &\quad + K_2\left([\theta]_{2\pi} - \pi\right)|x_4|\sin(\theta)\\ &= K_2\left([\theta]_{2\pi} - \pi\right)|x_4|\sin(\theta) \leq 0.\end{aligned}$$

This shows that $(\ell,\theta) = (0,\pi)$ is stable and $\Omega_\pi := \sup_{c\geq 0} V^{-1}(c)$ such that $\Omega_\pi \subset \mathbb{R}\times U_\pi$ is a compact positively invariant set.

To prove (iii) consider the set

$$E := \{(\ell,\ \theta)\in\Omega_0 : \dot V = 0\} = \{(\ell,\ \theta)\in\Omega_0 : |x_4|\theta = 0\}.$$

By assumption there exists a positive number $\epsilon > 0$ such that as $t\to\infty$, $|x_4| > \epsilon$. Under this observation we characterize the largest invariant set contained in E_0. For a solution to remain in E we must have that $\theta = 0$ and $\dot\theta = 0$. By the choice of control law (13), this means that $x_4\ell = 0$. Therefore the largest invariant set contained in E is given by $M = \{(\ell,\ \theta)\in E : x_4\ell = 0\}$. If $|x_4|\geq\epsilon$, then the invariance principle implies $(\ell,\theta)\to 0$. A similar argument applies to $(\ell,\theta) = (0,\pi)$.

□

In summary, the unicycle's control algorithm works as follows. In M, we feedback linearize the unicycle using the path following output to obtain (6) and apply the linear controller $v_a^{\pitchfork}$ in (11). In the singularity set M_δ, we switch to feedback transformation (9) with $v_\delta^{\pitchfork}$ defined in (13). If this switch occurs while on the path following manifold, the control $v_\delta^{\pitchfork}$ maintains controlled invariance of the path following manifold. Moreover, the switching has no effect on the tangential dynamics of the unicycle.

VI. Synchronization control design

We now design the tangential controllers $v_a^{\parallel}$, $v_b^{\parallel}$ to achieve **S**. The relevant tangential dynamics of $\Gamma_a^\star$ and $\Gamma_b^\star$ are

$$\begin{aligned}\dot\eta_1^a &= \eta_2^a \quad \dot\eta_1^b = \eta_2^b\\ \dot\eta_2^a &= v_a^{\parallel} \quad \dot\eta_2^b = v_b^{\parallel}.\end{aligned} \tag{15}$$

with state space $(\mathbb{R}\bmod L_a\times\mathbb{R})\times(\mathbb{R}\bmod L_b\times\mathbb{R})$. Physically, η_1^a and η_1^b represent the arc-length along the respective paths to the location of the output, while η_2^a and η_2^b govern the velocities along the paths. Let $\eta^a := (\eta_1^a,\eta_2^a)$, $\eta^b := (\eta_1^b,\eta_2^b)$ and define $\eta_1 := (\eta_1^a,\eta_1^b)$, $\eta_2 := (\eta_2^a,\eta_2^b)$.

Assumption 2. *System Σ_a has η^b available for feedback while Σ_b has η^a available for feedback. The synchronization constraint $F : \mathcal{C}_a\times\mathbb{R}^{p_a}\times\mathcal{C}_b\times\mathbb{R}^{p_b}\to\mathbb{R}^k$ is known to all.*

1) Position synchronization: Positional synchronization corresponds to a path following constraint (cf. Definition II.1) of the form $F : \mathcal{C}_a\times\mathcal{C}_b\to\mathbb{R}^k$. The set $\mathcal{C}_a\times\mathcal{C}_b$ is diffeomorphic to $\mathbb{R}\bmod L_a\times\mathbb{R}\bmod L_b$ which in turn is diffeomorphic to the 2-torus $\mathbb{T}^2$. These arguments show that $\mathcal{C}_a\times\mathcal{C}_b$ is a manifold of dimension 2 and hence $F : \mathcal{C}_a\times\mathcal{C}_b\to\mathbb{R}^k$ is restricted to have co-domain with $k\in\mathbf{2}$. If $k = 2$ then $F^{-1}(0)$ is a point on $\mathcal{C}_a\times\mathcal{C}_b$. The $k = 2$ case is uninteresting because it amounts to each system going to a particular point on its path. Such an objective can be solved easily, in light of the tangential dynamics (15), in a decentralized manner. If $k = 1$ then $F^{-1}(0)$ is an embedded submanifold. Instead of working with F, it convenient to instead work the function $G : \mathbb{R}\bmod L_a\times\mathbb{R}\bmod L_b\to\mathbb{R}^k$ uniquely defined by the diagram

$$\begin{array}{ccccc}\mathcal{N}(\mathcal{C}_a)\times\mathcal{N}(\mathcal{C}_b) & \xrightarrow{(\varpi_a,\varpi_b)} & \mathbb{R}\bmod L_a\times\mathbb{R}\bmod L_b & \xrightarrow{(\sigma_a,\sigma_b)} & \mathcal{C}_a\times\mathcal{C}_b\\ & & \searrow^{G} & & \downarrow F\\ & & & & \mathbb{R}^k.\end{array}$$

Synchronization is achieved at time t if $G(\eta_1^a(t),\eta_1^b(t)) = 0$.

Example VI.1. Consider the map $G : \mathbb{R}\bmod L_a\times\mathbb{R}\bmod L_b\to\mathbb{R}$ defined by

$$G_1(\eta_1^a,\eta_1^b) = \sin\left(\frac{2\pi}{L_b}\left[\eta_1^b - f(\eta_1^a)\right]_{L_b}\right) \tag{16}$$

where $f : \mathbb{R}\bmod L_a\to\mathbb{R}\bmod L_b$. For example $f(\eta_1^a) = \left[c_1\cos\left(\frac{2\pi}{L_a}\eta_1^a + c_2\right)\right]_{L_b}$ where $c_1, c_2\in\mathbb{R}$ are constants. This function equals zero when $\eta_1^b - f(\eta_1^a) = 0$ or $\eta_1^b - f(\eta_1^a) = \frac{L_b}{2}$. It corresponds to the position of Σ_b on its path being a periodic function of the position of Σ_a on its path. Figure 2 provides a visualization of this constraint on $\mathbb{R}\bmod L_a\times\mathbb{R}\bmod L_b$ and on the torus. Note that the level set $G^{-1}(0)$ has two connected components.

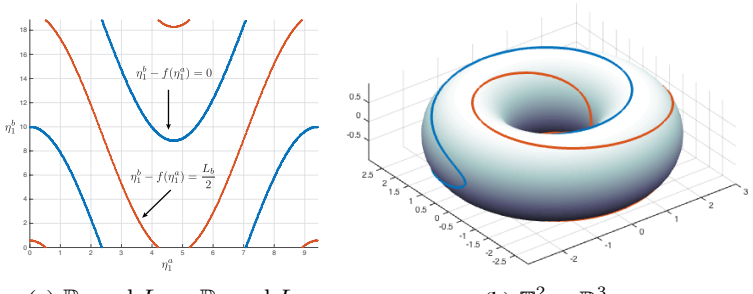

(a) $\mathbb{R}\bmod L_a\times\mathbb{R}\bmod L_b$. (b) $\mathbb{T}^2\subset\mathbb{R}^3$

Fig. 2: Zero level sets of (16) with $c_1 = 10$, $c_2 = 0$, $L_a = 3\pi$, $L_b = 6\pi$.

Another example is

$$G_2(\eta_1^a,\eta_1^b) = \sin\left(2\pi\left(\frac{c_1}{L_a}\eta_1^a - \frac{c_2}{L_b}\eta_1^b\right)\right). \tag{17}$$

If c_1, c_2 are commensurate then the zero level set of (17) corresponds to a closed curve on the torus. The zero level set again has two connected components which correspond to $\frac{c_1}{L_a}\eta_1^a - \frac{c_2}{L_b}\eta_1^b = 0$ and $1/2$.

The zero level set of

$$G_2(\eta_1^a, \eta_1^b) = (\eta_1^a - c_1)^2 + (\eta_1^b - c_2)^2 - r^2 \tag{18}$$

is a circle but G is not smooth as a function on the torus. However, if the constants c_1, c_2, r are chosen so that $G^{-1}(0) \subset (0, L_a) \times (0, L_b)$ then it is a permissible synchronization constraint. △

Next, we propose synchronization control laws. To begin with define synchronization error according to

$$e = \begin{bmatrix} e_1 \\ e_2 \end{bmatrix} \coloneqq \begin{bmatrix} G(\eta_1^a, \eta_1^b) \\ \frac{\partial G}{\partial \eta_1^a}\eta_2^a + \frac{\partial G}{\partial \eta_1^b}\eta_2^b \end{bmatrix}.$$

The e-dynamics are given by

$$\begin{aligned} \dot{e}_1 &= e_2 \\ \dot{e}_2 &= \begin{bmatrix} \eta_2^a & \eta_2^b \end{bmatrix} \operatorname{Hess}(G) \begin{bmatrix} \eta_2^a \\ \eta_2^b \end{bmatrix} + \mathrm{d}G \begin{bmatrix} v_a^{\parallel} \\ v_b^{\parallel} \end{bmatrix}. \end{aligned}$$

Select the tangential control law

$$\begin{bmatrix} v_a^{\parallel} \\ v_b^{\parallel} \end{bmatrix} = \begin{bmatrix} \frac{\nabla G}{\|\mathrm{d}G\|^2} & \frac{N(\eta_1)}{\|\mathrm{d}G\|^2} \end{bmatrix} \begin{bmatrix} -\eta_2^\top \operatorname{Hess}(G)\eta_2 + K_e e \\ v_s \end{bmatrix} \tag{19}$$

where $\nabla G = \mathrm{d}G^\top \in \mathbb{R}^2$, $N(\eta_1) \coloneqq R_{\frac{\pi}{2}} \nabla G$, $R_{\frac{\pi}{2}}$ is a $\pi/2$ counter-clockwise rotation of the plane, $K_e \in \mathbb{R}^{1\times 2}$ is a matrix of negative gains, and $v_s \in \mathbb{R}$ is an auxiliary control input to be designed so that the synchronized system has a desired motion while synchronized, i.e., restricted to $G^{-1}(0)$. This controller is well-defined as long as $\mathrm{d}G_{\eta_1} \neq 0$ which means, by the Morse-Sard theorem, it is well-defined except on a set of Lebesgue measure zero. In particular it is well-defined in a neighbourhood of $G^{-1}(0)$.

With this choice the closed-loop e-dynamics become

$$\begin{aligned} \dot{e}_1 &= e_2 \\ \dot{e}_2 &= K_{e,1} e_2 + K_{e,2} e_2 \end{aligned} \tag{20}$$

and, so long as $\mathrm{d}G \neq 0$, $e \to 0$ so that[3] $(\eta_a, \eta_b) \to \mathcal{S}^\star \coloneqq \{(\eta^a, \eta^b) : e_1 = e_2 = 0\}$.

Remark VI.1. *We stress that when $\xi^a = 0$ and $\xi^b = 0$ the systems Σ_a and Σ_b, respectively, evolve on their assigned paths $\mathcal{C}_a$ and $\mathcal{C}_b$. Meanwhile, under the control law (19), the set $\mathcal{S}^\star = \{(\eta^a, \eta^b) : e_1 = e_2 = 0\}$ is controlled invariant and locally attractive. On this set the positional synchronization constraint is enforced and the two systems are synchronized.*

To control the evolution of the overall system while synchronized we find an expression for the tangential dynamics (15) restricted to the set $\mathcal{S}^\star$.

Proposition VI.2. *The closed-loop tangential dynamics (15) under the control law (19) restricted to the set $\mathcal{S}^\star$ satisfy*

$$\eta_2(t)|_{\mathcal{S}^\star} = \frac{1}{\|\mathrm{d}G(t)\|^2} \langle N(\eta_1(t)),\ \eta_2(t) \rangle N(\eta_1(t)) \tag{21}$$

and

$$\dot{\eta}_2|_{\mathcal{S}^\star} = -\frac{\|\eta_2\|^2}{\|\mathrm{d}G\|^2} N^\top(\eta_1) \operatorname{Hess}(G) N(\eta_1) \frac{\nabla G}{\|\mathrm{d}G\|^2} + v_s \frac{N(\eta_1)}{\|\mathrm{d}G\|^2}. \tag{22}$$

Proof. On the set $\mathcal{S}^\star$, $\eta_2 \in \operatorname{Ker}(\mathrm{d}G)$. Since $N(\eta_1) = R_{\frac{\pi}{2}} \nabla G$ we have that $\operatorname{Ker}(\mathrm{d}G) = \operatorname{span}(N(\eta_1))$ which shows that η_2 is colinear with the unit vector $\frac{N(\eta_1)}{\|DG\|}$, i.e.,

$$\eta_2|_{\mathcal{S}^\star} = k(\eta_1, \eta_2) \frac{N(\eta_1)}{\|\mathrm{d}G\|}.$$

The function k is uniquely defined by the properties (i) $|k| = \|\eta_2\|$ and (ii) positive when $\eta_2/\|\eta_2\|$ and $N(\eta_1)/\|\mathrm{d}G\|$ are equal. The function

$$k(\eta_1, \eta_2) = \frac{1}{\|\mathrm{d}G\|} \langle N(\eta_1),\ \eta_2 \rangle$$

meets these requirements which shows that (21) holds. Lastly, since $e = 0$ when synchronized, direct substitution of (19) into (15) yields (22). □

Suppose we are given a desired velocity profile for the synchronized system. In light of Proposition VI.2 and (21), the desired velocity profile has the form

$$\eta_2^{\mathrm{ref}}(t) \coloneqq \mathrm{v}(t) \frac{N(\eta_1)}{\|\mathrm{d}G\|} \tag{23}$$

with $\mathrm{v} : \mathbb{R} \to \mathbb{R}$ smooth. Define the velocity tracking error

$$e_{\mathrm{v}} \coloneqq \frac{1}{\|\mathrm{d}G\|} \langle N(\eta_1),\ \eta_2 \rangle - \mathrm{v}. \tag{24}$$

Under the feedback (19), differentiating (24) we obtain

$$\begin{aligned} \dot{e}_{\mathrm{v}} = \left\langle \left(N \otimes \mathrm{d}\left(\frac{1}{\|\mathrm{d}G\|} \right) + \frac{1}{\|\mathrm{d}G\|} \mathrm{d}N_{\eta_1} \right) \eta_2,\ \eta_2 \right\rangle \\ + v_s \frac{1}{\|\mathrm{d}G\|} - \dot{\mathrm{v}}. \end{aligned} \tag{25}$$

The expression (25) does not require that (15) be restricted to $\mathcal{S}^\star$ as in Proposition VI.2; the evolution of the e_{v} dynamics (25) is decoupled from the synchronization error e. The expression (25) immediately suggests the control law

$$\begin{aligned} v_s = \|\mathrm{d}G\| \left(\dot{\mathrm{v}} - \left\langle \left(N \otimes \mathrm{d}\left(\frac{1}{\|\mathrm{d}G\|} \right) + \frac{1}{\|\mathrm{d}G\|} \mathrm{d}N_{\eta_1} \right) \eta_2,\ \eta_2 \right\rangle \right) \\ + K_{\mathrm{v}} \|\mathrm{d}G\| e_{\mathrm{v}}, \qquad K_{\mathrm{v}} < 0. \end{aligned} \tag{26}$$

Lemma VI.3. *Given $G : \mathbb{R} \bmod L_a \times \mathbb{R} \bmod L_b \to \mathbb{R}$ there exists an open set of initial conditions $U_1 \times U_2 \subseteq (\mathbb{R} \bmod L_a \times \mathbb{R} \bmod L_a) \times \mathbb{R}^2$ with $G^{-1}(0) \subset U_1$ such that for any initial condition $(\eta_1(0), \eta_2(0)) \in U_1 \times U_2$ the closed-loop tangential dynamics (15) under controllers (19) and (26):*

(i) *Achieve synchronization $G(\eta_1^a(t), \eta_1^b(t)) \to 0$.*
(ii) *The synchronized system tracks the desired velocity profile (23) $e_{\mathrm{v}} \to 0$.*
(iii) *The synchronization constraint is invariant, i.e., if $(\eta_1(0), \eta_2(0)) \in \mathcal{S}^\star$ then, for all $t \geq 0$, $(\eta_1(t), \eta_2(t)) \in \mathcal{S}^\star$.*

[3] Since the domain of G is compact, $G(\eta_1^a, \eta_1^b) \to 0$ if, and only if, $(\eta_1^a, \eta_1^b) \to G^{-1}(0)$.

Proof. Claims (i) and (iii) follow from the form the expression of the closed-loop synchronization error dynamics (20). Claim (ii) follows from the closed-loop velocity tracking error dynamics $\dot{e}_{\mathrm{v}} = K_{\mathrm{v}} e_{\mathrm{v}}$. □

Remark VI.4. *The controllers (19) and (26) ensure that the set $\mathcal{S}^\star$ is controlled invariant. Therefore, if the desired velocity profile $\mathrm{v} : \mathbb{R} \to \mathbb{R}$ changes in real-time, the systems will (a) stay on their paths (b) remain synchronized and (c) asymptotically track the new velocity profile. These features are unique to the proposed control laws.*

2) Velocity synchronization: Consider the special case where the path following synchronization constraint from Definition II.1 imposes a constraint on the velocities along the path. Analogously to the construction in Section VI-1, this can be viewed as a relation $G(\eta_2^a, \eta_2^b) = 0$ where $G : \mathbb{R}\times\mathbb{R} \to \mathbb{R}^k$, $k \in \mathbf{2}$, is smooth. As before, we assume that $k = 1$ to avoid the trivial case. We propose the tangential controllers

$$v_a^{\parallel} = K_a^{\mathrm{v}} \frac{\partial G}{\partial \eta_2^a} G(\eta_2^a, \eta_2^b),\ v_b^{\parallel} = K_b^{\mathrm{v}} \frac{\partial G}{\partial \eta_2^b} G(\eta_2^a, \eta_2^b),\ K_a^{\mathrm{v}}, K_b^{\mathrm{v}} < 0. \tag{27}$$

Lemma VI.5. *Given a velocity synchronization constraint $G : \mathbb{R}^2 \to \mathbb{R}$, there exists an open set of initial conditions $U_1 \times U_2 \subseteq (\mathbb{R} \bmod L_a \times \mathbb{R} \bmod L_a) \times \mathbb{R}^2$ with $G^{-1}(0) \subset U_2$ such that for any initial condition $(\eta_1(0), \eta_2(0)) \in U_1 \times U_2$ the closed-loop tangential dynamics (15) under the controller (27) are such that $G(\eta_2^a(t), \eta_2^b(t)) \to 0$ as $t \to \infty$. If G is proper then $\eta_2^a(t)$ and $\eta_2^b(t)$ are bounded.*

Proof. The synchronization constraint evolves according to

$$\begin{aligned}\frac{\mathrm{d}}{\mathrm{d}t} G &= \frac{\partial G}{\partial \eta_2^a} v_a^{\parallel} + \frac{\partial G}{\partial \eta_2^b} v_b^{\parallel} \\ &= \left(K_a^{\mathrm{v}} \left(\frac{\partial G}{\partial \eta_2^a} \right)^2 + K_b^{\mathrm{v}} \left(\frac{\partial G}{\partial \eta_2^b} \right)^2 \right) G.\end{aligned}$$

Since $K_u^{\mathrm{v}}, K_r^{\mathrm{v}} < 0$ and $\mathrm{d}G$ has rank 1 in a neighbourhood of $G^{-1}(0)$, $G(t)$ approaches 0 exponentially as $t \to +\infty$. Boundedness of η_2^b and η_2^b follows from the boundedness of G and the hypothesis that G is proper. □

Remark VI.6. *If G is a linear velocity constraint, i.e., $G(\eta_2^a, \eta_2^b) = g_1\eta_2^a + g_2\eta_2^b$, it is not proper. The conclusions of Lemma VI.5 still hold in this case except that boundedness is shown using the Lyapunov function $V(\eta_2^a, \eta_2^b) = -K_b^{\mathrm{v}}/2\,(\eta_2^a)^2 - K_a^{\mathrm{v}}/2\,(\eta_2^b)^2$.*

VII. Numerical example with model uncertainty

We implement the feedback linearization controllers using the path following output as well as (11), (19) and (26) for both systems. For the unicycle, when a singularity is encountered, we switch from the feedback linearizing controller to (9), (13). The model parameters for the manipulator are taken from [16] which provides a high accuracy model of a Clearpath® Robotic Manipulator whose shoulder, elbow, and wrist links are actuated by D.C. linear actuators.

A nominal manipulator model (2) is used for as the basis for control design. The simulated model has $\pm 1\%$ uncertainty on the motor inertias and damping and $\pm 0.5\%$ uncertainty on all masses associated with the manipulator. The latter respresenting severe modelling uncertainty. The unicycle is assigned an elipse

$$\mathcal{C}_a = \left\{ y_a : \frac{1}{a_1^2}\left(y_{a,1} - a_2\right)^2 + \frac{1}{a_3^2}\left(y_{a,2} - a_4\right)^2 - 1 = 0 \right\},$$

$\sigma_a(\lambda) = (a_1 \cos(\lambda) + a_2, a_3 \sin(\lambda) + a_4)$. The manipulator is assigned a limaçon-like curve $\mathcal{C}_b$ with smooth parameterization

$$\sigma_b(\lambda) = \begin{bmatrix} (b_1 + b_2\cos(\lambda))\cos(\lambda) + b_5 \\ (b_1 + b_2\cos(\lambda))\sin(\lambda) + b_6 \\ (b_3 + b_4\cos(\lambda))\cos(\lambda) + b_7 \end{bmatrix}.$$

The real constants a_i, $i \in \mathbf{4}$, and b_j, $j \in \mathbf{7}$ determine the properties of $\mathcal{C}_a$ and $\mathcal{C}_b$. We use[4] $a = (80, 0, 50, 500)$ and $b = (100, 50, 70, 100, 0, 500, 200)$ in this simulation so that $L_a \approx 413.8$, $L_b \approx 828.1$ where all distances are in millimetres. By Lemma III.2 the unicycle is feedback equivalent to (6), provided $x_4 \neq 0$. Similarly, by selecting the parameters b_j in $\sigma_b(\lambda)$ so that the path $\mathcal{C}_b$ does not pass through kinematic singularities of the manipulator, the manipulator is locally feedback equivalent to (7).

TABLE I: Controller parameters used in simulation

K_a, K_b	δ	K_{v}	K_e	K_1, K_2
$-\begin{bmatrix} 104 & 20 \end{bmatrix}$	0.3	-7	$-\begin{bmatrix} 10 & 6 \end{bmatrix}$	$1, \sqrt{2}$

Table I lists the gains and controller parameters used in simulations. The transversal gains K_a, K_b in (11) were selected using pole placement to ensure a fast approach to the paths with closed-loop poles at $s = -10 \pm j2$. The switching parameter δ was chosen to reduce the peak values of the unicycle's control signal. The remaining gains were chosen in an ad-hoc manner though LQR optimization or pole placement could be used to select the gain K_e that governs the synchronization error dynamics (20).

We simulate a case where the synchronization constraint switches to illustrate the unique features of our approach. For the first half of the simulation the constraint is (17) with $c_1 = c_2 = 1$. This represents the two systems traversing their respective paths together. At $t = 25$s the constraint switches to (18) with $c_1 = 200$, $c_2 = 400$, and $r = 100$. This constraint represents the two systems oscillating along their paths in a synchronized manner. The desired velocity for the synchronized systems is always $\mathrm{v}(t) = 50 + 25\cos(2\pi/10t)$.

Figure 3 shows typical output trajectories for both systems. Observe that both systems remain on their paths when the synchronization constraint is changed. Figure 4 shows the transversal states do not jump during the switch. This indicates that the robots do not leave their path due to switching. The invariance of the path is unique feature of path following controllers that make the path following manifold controlled invariant.

Figure 5 shows the phase plot η_1^a vs η_1^b of the tangential states. They converge to the initial constraint (a line) and then

[4]Where $a := (a_1, a_2, a_3, a_4)$ defines $\mathcal{C}_a$, similarly with b and $\mathcal{C}_b$.

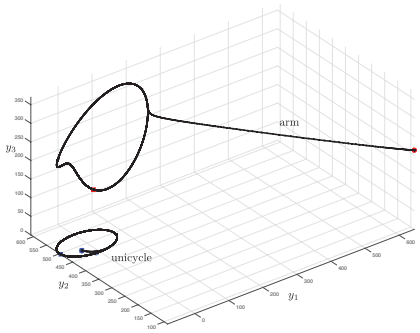

Fig. 3: Output trajectories $y_a(t)$ and $y_b(t)$.

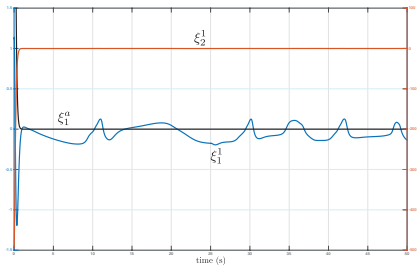

Fig. 4: Attractivity of paths despite model uncertainty.

at $t = 25$ s, when $G^{-1}(0)$ changes to a circle, they converge to the new synchronization constraint. This is further illustrated in Figure 6 where the value of G is plotted in blue for $t \leq 25$ and black for $t > 25$.

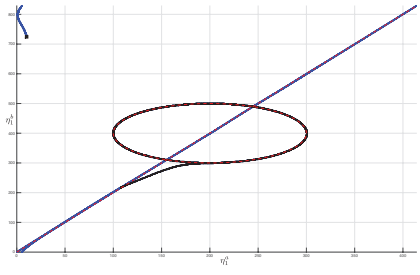

Fig. 5: η_1^a vs η_1^b.

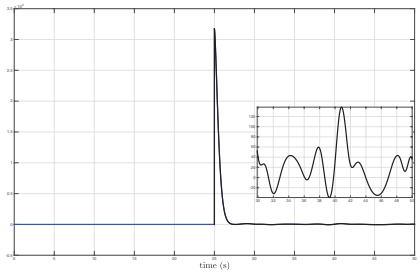

Fig. 6: $G(\eta_1^a(t), \eta_1^b(t))$ versus time.

Figure 7 shows that when the synchronization function changes, a transient is introduced to the velocity tracking error but the synchronized system quickly returns to tracking the assigned velocity profile $\mathrm{v}(t)$.

The model uncertainty manifests itself in the steady-state error in the synchronized velocity tracking (Figure 7). The steady-state velocity tracking error oscillates between $\pm 2\mathrm{mm/s}$. The model uncertainty is also noticeable in the steady-state value of the synchronization function $G(\eta_1^a(t), \eta_1^b(t))$. While these results are encouraging, the performance could be improved by employing Lyapunov redesign [16] or adaptive control.

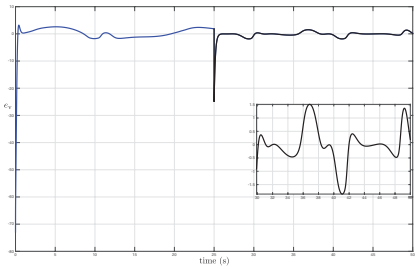

Fig. 7: Velocity tracking error (24).

REFERENCES

[1] A. P. Aguiar, J. P. Hespanha, and P. V. Kokotović, "Performance limitations in reference tracking and path following for nonlinear systems," *Automatica*, vol. 44, no. 3, pp. 598–610, 2008. 1

[2] C. Nielsen, C. Fulford, and M. Maggiore, "Path following using transverse feedback linearization: Application to a Maglev positioning system," *Automatica*, vol. 46, no. 3, pp. 585–590, 2010. 1, 3

[3] R. Ghabcheloo, A. Pascoal, C. Silvestre, and I.Kaminer, "Non-linear co-ordinated path following control of multiple wheeled robots with bidirectional communication constraints." *Int. J. Adapt. Control Signal Process*, no. 2-3, pp. 133—-157, 2007. 1

[4] A. Aguiar and A. Pascoal, "Coordinated path-following control for nonlinear systems with logic-based communication," in *IEEE Conf. on Decision and Control*, Dec. 2007, pp. 1473–1479. 1

[5] J. Ghommam and F. Mnif, "Coordinated path-following control for a group of underactuated surface vessels," *IEEE Trans. on Industrial Electronics*, vol. 56, no. 10, pp. 3951 –3963, oct. 2009. 1

[6] E. Børhaug, A. Pavlov, E. Panteley, and K. Pettersen, "Straight line path following for formations of underactuated marine surface vessels," *IEEE Trans. Control Systems Tech.*, vol. 19, no. 3, pp. 493–506, 2011. 1

[7] I.-A. F. Ihle, M. Arcak, and T. I. Fossen, "Passivity-based designs for synchronized path-following," *Automatica*, vol. 43, no. 9, pp. 1508–1518, 2007. 1

[8] R. Olfati-Saber and R. Murray, "Consensus problems in networks of agents with switching topology and time-delays," *IEEE Trans. on Automatic Control*, vol. 49, no. 9, pp. 1520–1533, 2004. 1

[9] A. Doosthoseini and C. Nielsen, "Coordinated path following for unicycles : A nested invariant sets approach," *Automatica*, vol. 60, pp. 17–29, Oct. 2015. 1

[10] M. El-Hawwary and M. Maggiore, "Reduction principles and the stabilization of closed sets for passive systems," *IEEE Trans. on Automatic Control*, vol. 55, no. 4, pp. 982–987, 2010. 1

[11] M. W. Spong and N. Chopra, "Synchronization of networked lagrangian systems," in *Lagrangian and Hamiltonian Methods for Nonlinear Control 2006*, ser. Lecture Notes in Control and Information Sciences. Springer Berlin Heidelberg, 2007, vol. 366, pp. 47–59. 1

[12] S.-J. Chung and J.-J. Slotine, "Cooperative robot control and concurrent synchronization of Lagrangian systems," *IEEE Trans. on Robotics*, vol. 25, no. 3, pp. 686–700, 2009. 1

[13] Y. Li and C. Nielsen, "Position synchronized path following for a mobile robot and manipulator," in *IEEE Conf. on Decision and Control*, 2013, pp. 3541–3546. 1

[14] C. de Wit, B. Siciliano, and G. Bastin, Eds., *Theory of Robot Control*, ser. Communications and Control Engineering. Springer, 1996. 2, 3, 4

[15] L. Consolini, M. Maggiore, C. Nielsen, and M. Tosques, "Path following for the PVTOL aircraft," *Automatica*, vol. 46, no. 8, pp. 1284–1296, 2010. 4

[16] R. Gill, D. Kulić, and C. Nielsen, "Spline path following for redundant mechanical systems," *IEEE Trans. on Robotics*, vol. 31, no. 6, pp. 1378–1392, 2015. 7, 8